energies

MDPI

Article

Coupling Chemical Heat Pump with Nuclear Reactor for Temperature Amplification by Delivering Process Heat and Electricity: A Techno-Economic Analysis

Aman Gupta [1,2], Piyush Sabharwall [2], Paul D. Armatis [3], Brian M. Fronk [3] and Vivek Utgikar [1,*]

[1] Department of Chemical and Biological Engineering, University of Idaho, Moscow, ID 83844, USA
[2] Idaho National Laboratory, Idaho Falls, ID 83415, USA
[3] School of Mechanical, Industrial and Manufacturing Engineering, Oregon State University, Corvallis, OR 97331, USA
* Correspondence: vutgikar@uidaho.edu

Abstract: The energy economy is continually evolving in response to socio-political factors in the nature of primary energy sources, their conversions to useful forms, such as electricity and heat, and their utilization in different sectors. Nuclear energy has a crucial role to play in the evolution of energy economy due to its clean and non-carbon-emitting characteristics. A techno-economic analysis was undertaken to establish the viability of selling heat along with electricity for an advanced 100 MW_{th} small modular reactor (SMR) and four nuclear hybrid energy system (NHES) configurations featuring the SMR paired with chemical heat pump (ChHP) systems providing a thermal output ranging from 1 to 50 MW_{th}. Net present value, payback period, discounted cash flow rate of return, and levelized cost of energy were evaluated for these systems for different regions of U.S. reflecting a range of electricity and thermal energy costs. The analysis indicated that selling heat to high temperature industrial processes showed profitable outcomes compared to the sale of only electricity. Higher carbon taxes improved the economic parameters of the NHES alternatives significantly. Providing heat to high temperature industries could be very beneficial, helping to cut down the greenhouse gases emission by reducing the fossil fuel consumption.

Keywords: chemical heat pump; techno-economic; nuclear energy; temperature boost; industrial thermal processes

Citation: Gupta, A.; Sabharwall, P.; Armatis, P.D.; Fronk, B.M.; Utgikar, V. Coupling Chemical Heat Pump with Nuclear Reactor for Temperature Amplification by Delivering Process Heat and Electricity: A Techno-Economic Analysis. *Energies* **2022**, *15*, 5873. https://doi.org/10.3390/en15165873

Academic Editors: Janusz Badur and Tomasz Kowalczyk

Received: 13 July 2022
Accepted: 9 August 2022
Published: 13 August 2022

1. Introduction

The world faces a new challenge in the twenty-first century: that of lowering greenhouse gas emissions substantially while simultaneously providing energy access and economic opportunity to billions of people. During the recent United Nations Climate Change Conference of the Parties (COP26), a total of 137 countries, including China, United States, and India, have committed to net zero, carbon neutrality, or being climate neutral. To have a major impact on GHG emissions, non-electric energy sectors' (industry, commercial, residential, and transportation) carbon footprint must be decreased for achieving long-term emission reduction targets.

Researchers have been attracted to the integrated energy systems (IESs) in recent years due to their potential to reduce GHG emissions, improve energy efficiency, and electrical grid dependability, and enhance energy economics. IESs are collaboratively controlled systems that can dynamically apportion thermal and/or electrical energy to promote the production of various energy products while also providing responsive generation to the power grid. Multiple subsystems make up an IES, which may or may not be geographically co-located [1,2]. IES configurations are likely to help nuclear energy overcome its primary challenge, cost, which has resulted in the relatively limited expansion of nuclear power according to a recent MIT Future of Nuclear report [3]. In order to realize the benefits

of integrated nuclear-renewable energy systems (INRESs) with the current reactor fleets enabling them to provide process heat and improve economics as shown in Figure 1, selection and development of a complimentary temperature upgrading technology is necessary. Thermal energy can be used to generate power, be stored for later conversion to electricity, or be used in industrial thermal processes. In response to changing electric market conditions, this energy distribution can be modified to maximize the value of the IES. Solar thermal and nuclear power are becoming less appealing to investors as the price of electricity fluctuates due to the prioritization of renewable energy sources such as solar photovoltaic electricity and wind power. These high temperature energy generators facilities minimize greenhouse gas emissions, but they come with high upfront investments that are difficult to recoup rapidly in a fluctuating energy market. While thermal energy storage at times of lower electricity demand and later conversion to power under high demand conditions is a component of the solution, there is also a chance to sell heat instead of power when it is more profitable.

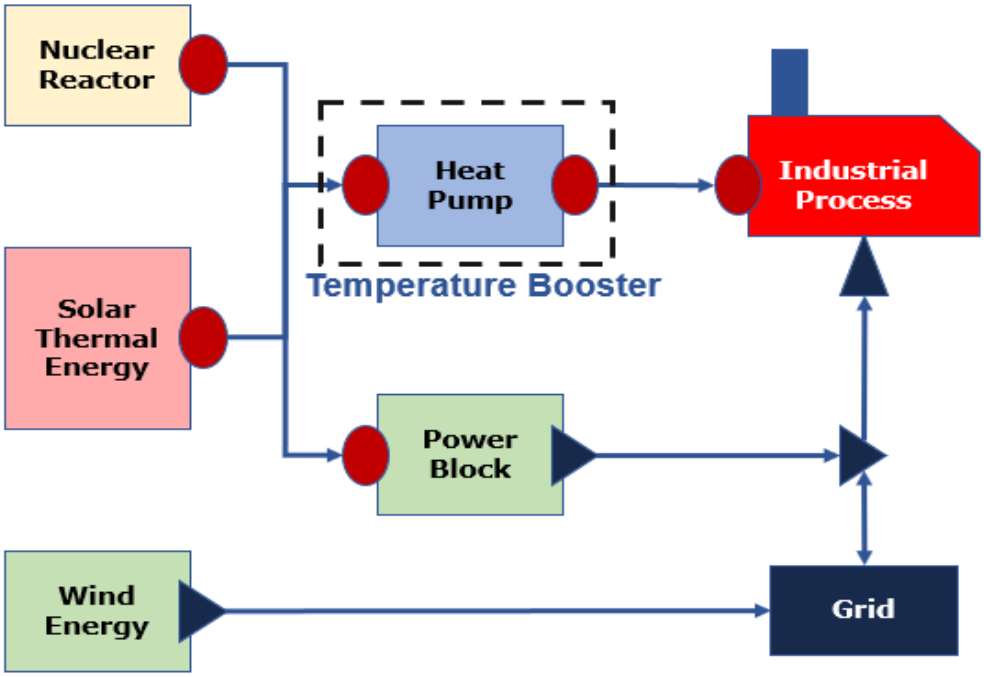

Figure 1. Example of Integrated Energy System.

McMillan et al. [4] gathered data on thermal energy consumption and CO_2 emissions for high-temperature thermal process businesses in the United States in 2016. They discovered that boilers or combined heat and power accounted for 70% of the 51 TBtu consumed in the US industrial sector in 2014, while direct process heating accounted for another 24%. Fossil fuels (mainly natural gas) are readily available, affordable, and simple to utilize; therefore, they are commonly used to generate the requisite high temperature heat. Instead of fossil fuels, using nuclear or renewable thermal energy for these applications can significantly reduce greenhouse gas (GHG) emissions. This also opens the possibility of using energy sources other than electricity, which isn't always feasible due to fluctuating electricity prices. Conventional nuclear reactors operate at 300–325 °C, whereas the high temperature thermal industrial processes typically require heat at greater than 550 °C as shown in Figure 2. To address the temperature mismatch, a heat pump is used between the nuclear power plant and the desired high temperature needed by industrial process.

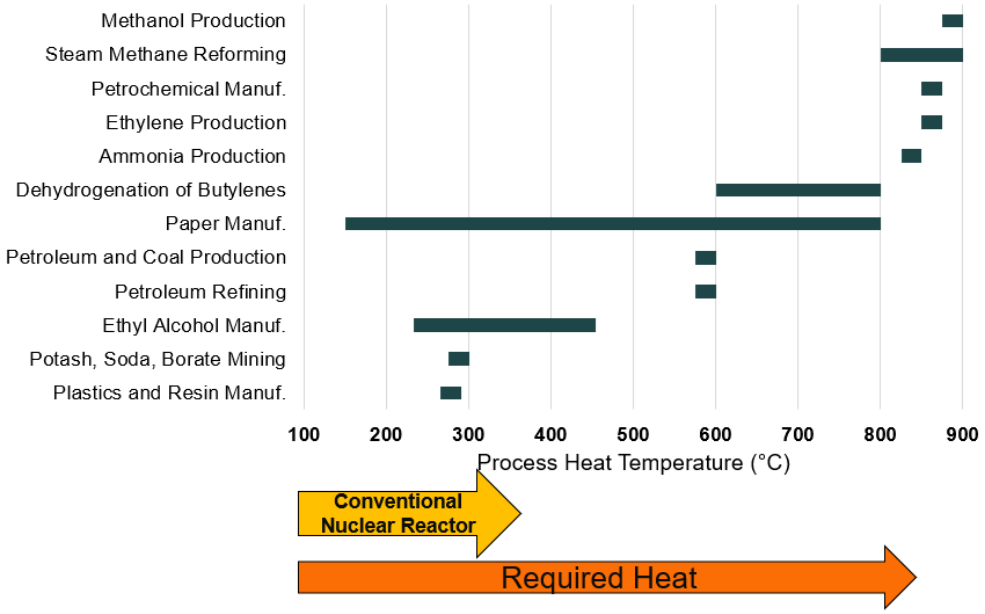

Figure 2. High Temperature Industrial Thermal Processes with Temperature Requirements [4].

Heat pump technologies are preferable to other alternatives (resistance heating) for achieving higher temperatures because they avoid the efficiency penalty associated with the thermal to electrical energy conversion while still enabling storage of thermal energy for later conversion to electricity if desired. Chemical heat pumps (ChHPs) are systems that use reversible chemical reactions to change the output temperature of the primary energy source. ChHP systems are characterized by high capacity, long term storage, and low energy loss [5]. Compared to mechanical or absorption heat pumps, ChHPs are capable of much higher temperature lifts and with significantly less mechanical input [6].

The operation of this system can be described in two basic steps: charging and discharging as shown in Figure 3 with schematic of the component and Clausius–Clapeyron diagram for the ChHP system based on $Ca(OH)_2/CaO$ system featuring cyclic dehydration-hydration reactions. In a survey conducted in 2013 by Sabharwall et al. [7], the reversible $Ca(OH)_2/CaO$ reaction shown in Equation (1) was established as the best candidate for high temperature boosting of heat from light water reactors to high temperature industrial thermal processes. The $Ca(OH)_2/CaO$ reaction has a high energy density, fast reaction kinetics, and an equilibrium curve appropriate for the high temperatures involved with the industries of interest. Energy charging starts with the addition of heat at T_M to dehydrate the chemical bed consisting of $Ca(OH)_2$ at low pressure. The vapor is then captured in a condenser and heat is rejected at T_C, usually the ambient temperature. For discharge, the vapor pressure is increased, and the condensed water is evaporated with heat added at T_E. The vapor then hydrates the chemical bed of CaO, releasing the stored heat at T_H. The completion of cycle positions the chemical bed for the energy charging step again. The heat input and rejection temperatures of a chemical heat pump are mainly dictated by the saturation or equilibrium temperatures of the refrigerant or reactants used. The calcium oxide hydration reaction has the potential to receive heat at 350 °C during charging and deliver heat above 600 °C during discharge. This means this reaction is not only helpful in delivering heat at high temperatures, but also providing temperature lifts greater than 250 °C. High temperature operation and large temperature lifts make the $CaO/Ca(OH)_2$ chemical heat pump a great candidate for efficient high temperature process heating using low-carbon thermal energy.

$$Ca(OH)_2(s) + \Delta H_r \rightleftharpoons CaO(s) + H_2O(g) \quad (1)$$

$$\Delta H_r = 104.4 \text{ kJ mol}^{-1}$$

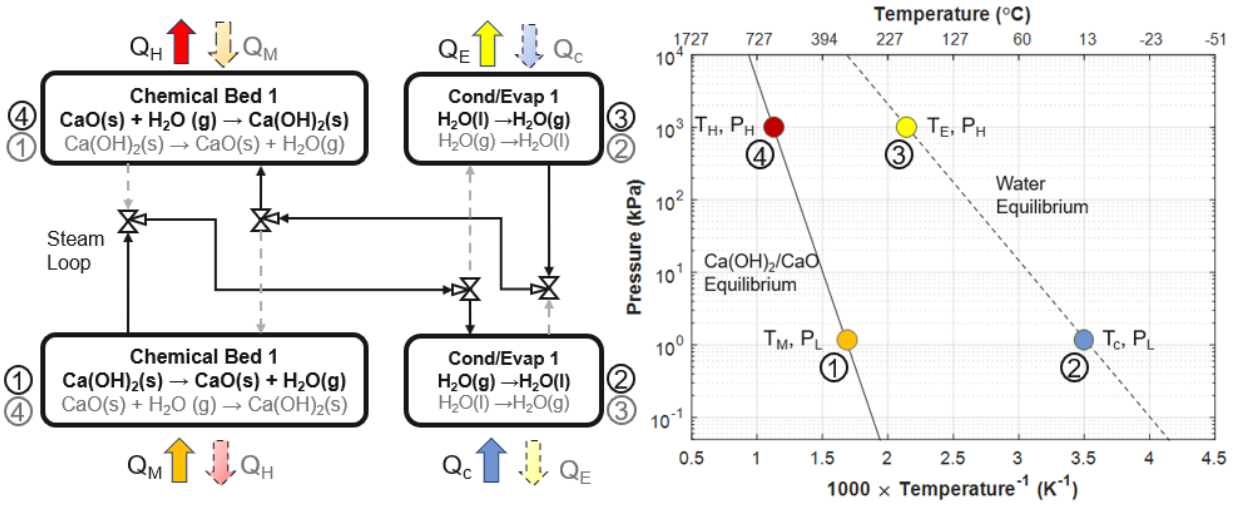

Figure 3. Schematics of components of $Ca(OH)_2/CaO$ ChHP system; Clausius–Clapeyron diagram (①–④ are the reaction conditions corresponding to the figure on the left).

Several researchers have investigated the feasibility of the $Ca(OH)_2/CaO$ reversible system both theoretically and experimentally [8–17]. These studies have been conducted on small scale (<1 g) to laboratory scale (60–2500 g) systems in a fixed bed reactor with direct and indirect heating. Modifying the reactant to improve its mechanical and physical properties has been the topic of a few recent investigations as studies have found agglomeration of reactant giving rise to low effective thermal conductivity and poor heat and mass transfer [18–23]. According to Roßkopf et al. [21,22], adding a minimal amount of nano-SiO2 to CaO particles prevented agglomeration and stabilized the bulk characteristics of CaO particles, but had little effect on lowering the dehydration temperature. Gupta et al. [23] investigated the effect of addition of CaTiO3 with $Ca(OH)_2$ pellets and the results showed increase in rate of reaction with 55% increase in mechanical strength of the pellet.

There have been very few studies focusing on the economic feasibility of ChHPs due to low technology readiness level (TRL) of the system. Spoelstra et al. [24] studied the techno-economic analysis of isopropanol-acetone and ammonia-salt ChHPs system for temperature amplification less than 150 °C. The ammonia–salt vapor heat pump, on the other hand, outperforms the isopropanol–acetone heat pump in terms of technical performance by evaluating internal rate of return of 7%, as it has a higher enthalpic efficiency and a higher coefficient of performance. Karaca et al. [25] investigated economics of ChHP based on ethanol–formaldehyde–hydrogen, ethanol–acetaldehyde–hydrogen, iso-propanol–acetone–hydrogen, and n-butanol–butyraldehyde–hydrogen systems for low temperature heat upgrade from 77–200 °C. These studies were conducted in 2002, and the economy and policy have changed significantly since then. Bayon et al. [26] explored the techno-economic feasibility of thermochemical energy storage systems when coupled with solar thermal energy. The working pair investigated were molten salts, alkaline-hydroxides, carbonates, and oxides. Of the 17 working pairs analyzed, 8 showed high potential for commercial applications with a cost lower than USD25 MJ^{-1} including $Ca(OH)_2/CaO$ system. There have not been any techno-economic studies reported which focus on ChHP for thermo-amplification to boost the temperature from 350 °C to greater than 600 °C.

The development of a SMR involves significantly less upfront money, resulting in lower financial risks and making it a viable alternative to large nuclear reactors (1 GW). An SMR can also combine with an integrated energy system to manage fluctuations in intermittent renewable energy generation while also storing energy or providing electricity/heat. Bolden et al. [27,28] examined the SMR economics through a comprehensive model based on first-of -a-kind (FOAK) through nth-of-a-kind (NOAK). The model evaluates a project's feasibility in regard to market conditions and commonly used capital budgeting techniques like the net present value (NPV), internal rate of return (IRR), payback period (PBP), and

the levelized cost of energy (LCOE). Sabharwall et al. [29] conducted a study on nuclear renewable energy integration economics comparing the economics of three cases nuclear, nuclear-wind, and nuclear-wind-hydrogen for PJM and Mid-C US markets. Nuclear–wind–hydrogen was the profitable case out of the three based on the assumptions of their study. Alonso et al. [30] conducted economic comparative study on SMR versus coal and combined cycle plants. They performed sensitivity analysis showing how NPV and IRR varies by changing discount rates and overnight capital cost. Within integrated energy systems, there is an obvious requirement to resolve temperature mismatches between energy sources and demands in the most effective way feasible. The techno-economics model is critical for determining whether technical and market factors make the coupling of a heat pump to a SMR advantageous and appealing to investors. A related techno-economic study from our research group focuses on identifying the number of profitable scenarios of chemical absorption heat pump–SMR system for upgrading nuclear heat when compared to advanced SMR based on PJM region hourly utility data for different years. The effect of chemical bed thermal conductivity and relative size of heat pump on economic metrics were also investigated [31].

The environmental benefits of SMR–heat pump systems over using fossil fuels for process heating are readily apparent. However, the economics of the system needs to be assessed in order to decide whether the system is a viable investment. This study focuses on economic feasibility of an SMR by selling electricity and nuclear hybrid energy system (NHES) i.e., SMR coupled with ChHP system by selling a combination of heat and electricity. For the techno-economic analysis, the average selling price of electricity and natural gas (for heat) for six different U.S regions are used. The ChHP specific capital cost is calculated using steady state thermodynamic model as there are no studies presently available which reported the specific cost of $Ca(OH)_2/CaO$ ChHP. The economic viability is compared by estimating the economic indicators such as net present value (NPV), payback period (PBP), discounted cash flow rate of return (DCFR), and levelized cost of energy (LCOE) for SMR and NHES systems.

2. Methodology

The general methodology used to assess the techno-economic feasibility of a system is shown in Figure 4. The first stage is to estimate the capital costs of the system. In next step, possible market and utility factors are evaluated. Finally, the necessary economic indicators are calculated to determine the techno-economic feasibility of the system or project. This section describes the evaluation of economic indicators, specific capital cost and baseline schematic of ChHP with SMR.

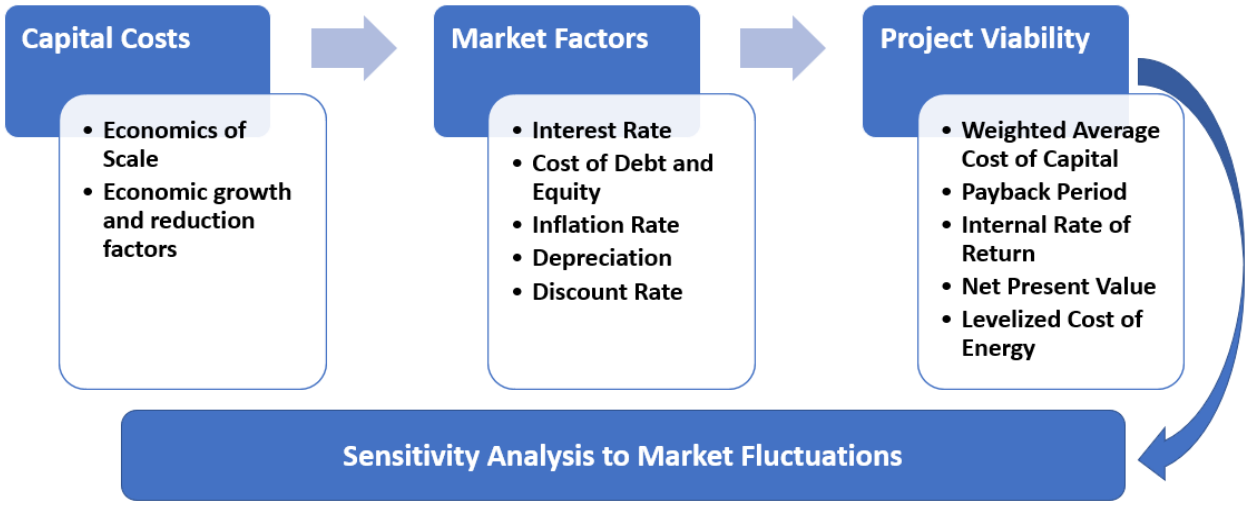

Figure 4. Overview of techno-economic analysis.

2.1. Baseline ChHP Coupled SMR System

The schematic of the baseline model used in this study is shown in Figure 5, where a ChHP is integrated with advanced an SMR to deliver heat to high temperature thermal industrial processes. This flow sheet shows the major components of the techno-economic model. The system uses thermal energy from the advanced SMR via molten salt as heat transfer fluid and delivers it to chemical bed which contains $Ca(OH)_2$ for the dehydration process. In the dehydration bed, $Ca(OH)_2$ decomposes into CaO in an endothermic reaction liberating water vapor. The molten salt returns back from the dehydration bed and is reheated in a closed loop. The liberated water vapor from dehydration bed is condensed in a condenser. At the same time a high-pressure steam from the evaporator is pumped to chemical bed 2 which reacts with CaO to form $Ca(OH)_2$ in an exothermic reaction. This is the hydration step and the temperature in the hydration bed is higher than the temperature in the dehydration bed. According to Clausius–Clapeyron equilibrium relation, higher pressure dictates the higher temperature. The heat from the hydration bed is removed using molten salt which is sent to the high temperature thermal industrial processes. This salt is again sent back to the hydration bed. This process is a continuous, and once the bed is dehydrated, it is ready for hydration and vice-versa.

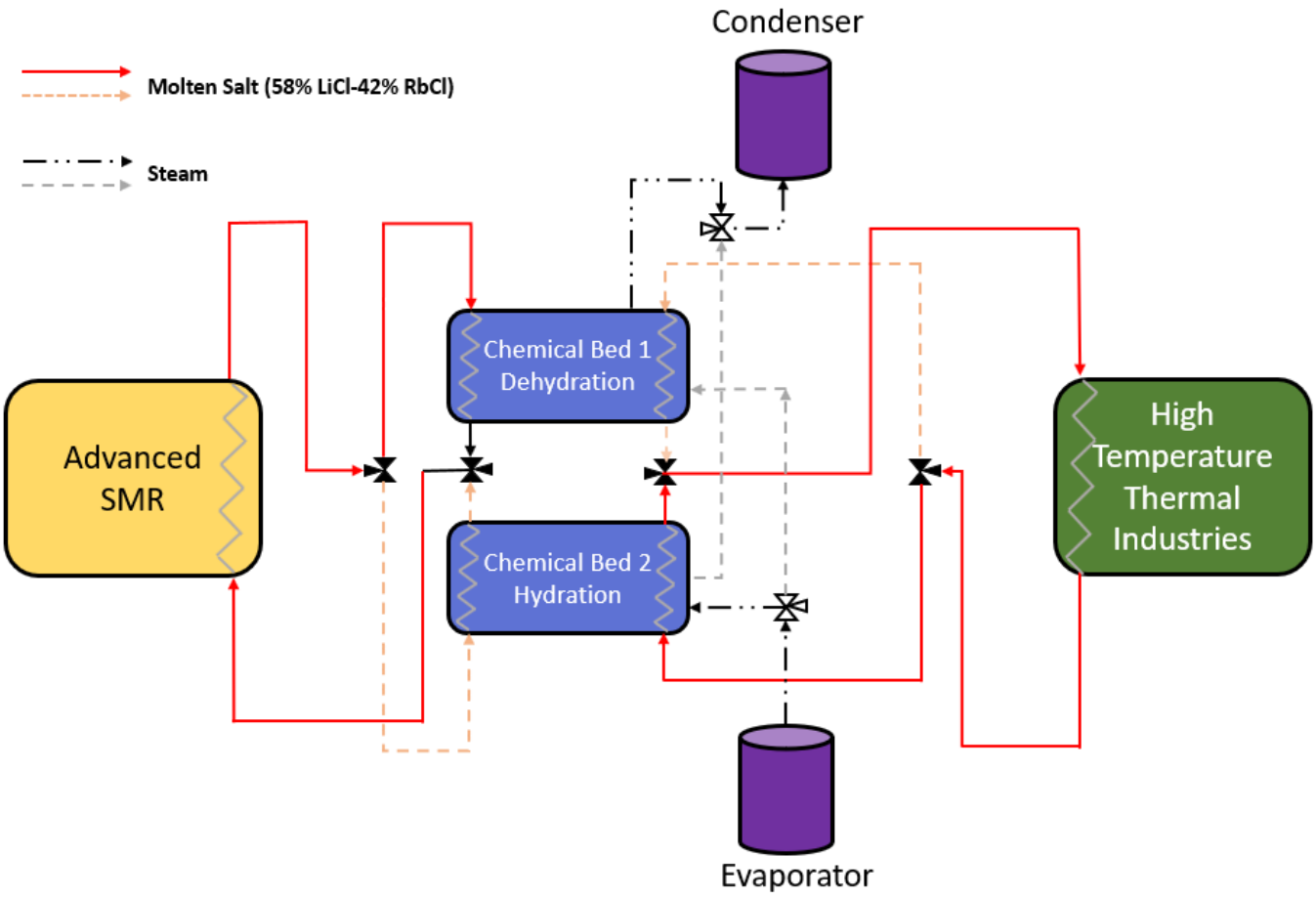

Figure 5. Schematic of ChHP coupled with SMR system.

The study focuses on an advanced SMR with a thermal output of 100 MW_{th} and a temperature output of 400 °C. The dehydration occurs at 380 °C and during hydration the molten salt temperature reaches to 650 °C for this study. The conventional light water SMR operates at 300–325 °C making the reaction kinetics slow due to that reason dehydration temperature assumed in this study is slightly higher.

2.2. Assessment of Capital Cost of System

The estimation of advanced SMR cost and ChHP are both required for techno-economic analysis of the system. Many studies have reported the capital cost of the advanced SMR. Sabharwall et al. [29] estimated the overnight capital cost (*OCC*) of SMR of USD4637/kW_e. Richards et al. [32] estimated the overnight specific capital cost of the molten salt reactors between USD2000 to USD3846/kW_e. A study conducted by MIT [3] assessed the overnight capital cost for NOAK reactors between USD3797 to USD6880/kW_e based on different design. FOAK SMRs overnight capital costs were projected with 10th-of-a-Kind estimates in a recent report Stewart et al. [33]. FOAK SMRs can range in price from USD4500 to USD8500/kW_e depending on the reactor type. After ten reactors, the price range can be reduced to USD3000–USD5000/kW_e as per NOAK model. For this study, an overnight capital cost of USD4637/kW_e is assumed and a parametric study is also conducted assuming overnight capital cost ranging from USD4500 to USD6500/kW_e. According to Boldon [27], the total specific capital cost (*TSCC*) can be computed by including the contingency cost rate (*CC*), detailed design and engineering cost rate (*DD&E*) and the overnight capital cost as shown in Equation (2). For this study, both the cost rates (*CC* and *DD&E*) were assumed to be 5%.

$$TSCC = OCC(CC + DD\&E + 1) \quad (2)$$

For the capital cost of $Ca(OH)_2$/CaO ChHP, there are no estimates available in literature. The capital cost of ChHP is estimated using a fundamental bottom-up approach assuming the reactor to have a shell and tube heat exchanger configuration. The chemical beds are projected to be the biggest and most costly components in the ChHP system, based on our earlier work [34]. The cost of the reactor was then estimated from the heat transfer area requirement. The specific cost of chemical bed based on heat transfer is assumed to be ranging from USD400–USD600/ft^2 as per quotation provided by a vendor of the heat exchange equipment, CG Thermal [35]. The heat transfer area needed for obtaining the cost was estimated by the approach used in our previous work [34].

The molten salt convective heat transfer resistance, the CaO/$Ca(OH)_2$ contact resistance, and the CaO/$Ca(OH)_2$ conduction resistance are used to estimate the overall heat transfer coefficients for dehydration and hydration reaction. Dittus–Boelter correlations were used to compute the dehydration and hydration convective heat transfer coefficients. The heat transport from the reaction steam in the bed via convection and radiation, as well as tube conduction resistance, is assumed negligible. The thermal conductivity of the $Ca(OH)_2$/CaO was calculated to be between the range of 0.1–0.55 W/mK and for this study it is assumed to be 0.5 W/mK [11]. Based on Linder et al. [36] work, the contact resistance is assumed to be 0.147 m^2K/kW. After estimating heat transfer area required for a single bed, the total capital cost of the ChHP chemical bed was calculated by using the Equation (3) where n_{bed} is number of total chemical bed and $bed_{s,cost}$ specific cost of bed based on heat transfer area (USD/m^2) which is assumed to be USD400/ft^2 [35].

$$cost_{bed} = A_{HT} n_{bed} bed_{s,cost} \quad (3)$$

The main contributor to the capital cost of the ChHP is the chemical beds. Chemical bed capital cost was assumed to be 90% of the total purchased cost of the ChHP system, and other costs included condenser, evaporator, and pump cost, which is assumed to be within the 10% of the total purchased cost. The purchase price of the equipment is only a percentage of the entire investment and other costs are involved in the construction of a facility which are summarized in Table 1. The total capital investment can be calculated using cost estimates for acquired equipment and expected proportions for each category. Based on Peters et al. [37], total capital investments were modified for ChHP system and were adjusted for the total sum to be 100%. Component costs can be estimated based on a size metric specific to the type of component. There may also be scale factors to account for materials and operational pressures. The majority of the component costs were estimated using cost curves from Peters et al. [37], with some data derived from steady-state point

models from our previous study [34]. Any error in this estimate is considered negligible. The main contributor to the capital cost of the ChHP is the chemical beds.

Table 1. Total Capital Investment Portion.

Category	Assumed Total Capital Investment %	Adjusted Total Capital Investment %
Purchased Equipment	50	46.29
Equipment Installation	10	9.25
Instrumentation	6	5.55
Piping	8	7.40
Electrical	3	2.77
Buildings	2	1.85
Yard Improvements	2	1.85
Service Facilities	8	7.40
Land	1	0.92
Engineering and Supervision	5	4.62
Construction Expenses	5	4.62
Legal Expenses	1	0.92
Contractor's Fee	2	1.85
Contingency	5	4.62

2.3. Economic Indicator Estimates

To study the techno-economic feasibility of the system described above, the economic indicators are evaluated which include payback period (*PBP*), net present value (*NPV*), discounted cash flow rate of return (*DCFR*), and levelized cost of energy (*LCOE*) as explained below.

2.3.1. Payback Period

The payback period (*PBP*) is the length of time required to recoup the funds expended in an investment, or to reach the break-even point and is calculated using the following Equations (4)–(6) where *PBP* is the payback period, V denotes the fixed capital investment, $\overline{A}$ denotes the average yearly cash flow over the project's lifetime, A_j is the annual cash flow or annuity in year j, N denotes the project's length in years, s represents sales, c_0 represents cost, d represents depreciation, Φ represents the corporate tax rate and j denotes a specific year [37].

$$PBP = \frac{V}{\overline{A}} \tag{4}$$

$$\overline{A} = \frac{1}{N}\sum_{j=1}^{N} A_j \tag{5}$$

$$A_j = \left(s_j - c_{o,j} - d_j\right)(1-\phi) + d_j \tag{6}$$

Compounding and discounting effects do not apply in this calculation since the payback period does not include the time worth of money. If a proposed investment's payback period is smaller than or equal to that of an existing solution for the same application, it may be worthwhile to pursue. If not, more investigation is required.

The concept of depreciation d is based upon the fact that physical facilities deteriorate and decline in usefulness with time thus, decreasing the values of the facility. There are several ways to estimate the depreciation rate, of which the Modified Accelerated Cost Recovery System (MACRS) is used in this study. With MACRS, a recovery period is selected based on the type of facility and a correlation is applied. These rates are based on average recovery period by IRS 2021 [38]. For power plants, a 15-year recovery period is commonly assumed [37].

In this study, the advanced SMR system produces and sells electricity and the combined advanced SMR and ChHP produce and sell both thermal energy and electricity at

natural gas and electricity prices, respectively. The utility price of thermal energy (heat) includes carbon tax in addition to the natural gas prices. For the electricity only case, the annual sales were evaluated using the Equation (7). The heat engine efficiency (η) for electricity generation was assumed to be 34%. The capacity factor (*CF*) was assumed to be 90% based on Sabharwall et al. [29] study. $\dot{Q}_{SMR}$ is the nominal heat generated by the advanced SMR and SP_e is the selling price of electricity.

$$s_{j,SMR} = \eta \cdot CF \cdot \dot{Q}_{SMR} \cdot SP_e \cdot 8760\ hrs \tag{7}$$

For the combined advanced SMR-ChHP system, which provides and sells both electricity and heat to the market, a carbon tax was added to the natural gas prices to estimate the selling price of heat. The annual sales for the combined advanced SMR-ChHP system are given by Equation (8) where SP_{ht} is the selling price of heat (combined natural gas and carbon tax prices), $\dot{Q}_{ChHP,in}$ is the heat rate from SMR to ChHP and $\dot{Q}_{ChHP,out}$ is the rate of thermal out energy from ChHP.

$$s_{j,SMR-ChHP} = \left(\left(\eta \cdot CF \cdot \left(\dot{Q}_{SMR} - \dot{Q}_{ChHP,in}\right) \cdot SP_e\right) + \left(CF \cdot \dot{Q}_{ChHP,out} \cdot SP_{ht}\right)\right) \cdot 8760\ hrs \tag{8}$$

The annual costs are calculated using the Equation (9) where the specific and fixed cost of operation and maintenance for the advanced SMR are represented by $O\&M_{spec}$ and $O\&M_{fix}$, respectively. The specific fuel cost of the uranium is represented by $Fuel_{spec}$. The values assumed for this study are described in detail in Section 2.4 for different cases and scenarios.

$$c_0 = \eta \cdot \dot{Q}_{SMR} \cdot \left(O\&M_{spec} + Fuel_{spec}\right) \cdot 8760\ hrs + O\&M_{fix} \cdot 1\ yr \tag{9}$$

2.3.2. Net Present Value

Net present value (*NPV*), also known as net present worth, is the difference between the present value of cash inflows and the present value of cash outflows over the lifetime of the plant [36]. The 'present' year identification is fairly arbitrary, and we choose the first year of the plant operation to be present. NPV accounts for the time value of money and is estimated using the following Equation (10).

$$NPV = \sum_{j=1}^{N} PWF_{cf,j}(A_j + rec_j) - \sum_{k=1}^{Nc} PWF_{v,k}\text{Ŧ}_k \tag{10}$$

$$PWF_{cf,j} = (1+i)^{-j} \tag{11}$$

$$PWF_{v,k} = (1+i)^{N_c - k} \tag{12}$$

The *rec* is the cost recovered from salvaged components, Ŧ is the investment cost and N_c is the construction time in years. Equation (11) represents the present worth factor for the annual cash flows. This factor discounts future cash flows where *i* is the discount rate. The same rate *i* can be assumed for the present worth factor in Equation (12) which compounds past investments. Both factors adjust the value of the money from past or future value to the present value. The cost recovered was assumed to be zero for this analysis.

$$i = \frac{WACC + 1}{r_{inf} + 1} - 1 \tag{13}$$

The discount rate *i* is an interest rate that provides the current worth of future money as shown in Equation (13) from Boldon [28]. A nominal discount rate includes inflation, while the real discount rate does not. The assumed inflation rate is expressed as r_{inf} and *WACC* is the weighted average capital cost, calculated in Equation (14) [28]. The *WACC* is a value describing the percentage of capital that must be paid to the investors, so they see the

expected return on investments/assets. The *WACC* may be affected by many factors, such as political and financial risks. C_d and C_{eq} represent the rate charged for costs of capital and equity, respectively. p_d and p_{eq} represent the portions of debt and equity for the project.

$$WACC = (p_d \times C_d) + (p_{eq} \times C_{eq}) \tag{14}$$

The portion of debt and charge rate of debt were assumed for the analysis. The portion of equity is just the portion left over that was not financed *(1-p_d)*. The rate charged for cost of equity is evaluated using the Equation (15) from Boldon [28] where Φ is the corporate tax rate which is assumed.

$$C_E = C_D(1 - \phi) \tag{15}$$

Based on study by Alonso et al. [30] the construction period of 3 years was assumed and constriction schedule for advanced SMR was assumed to be 60%, 20% and 20% for 1st, 2nd and 3rd year, respectively. ChHP construction schedule is assumed to be 0%, 20% and 80% for 1st, 2nd, and 3rd year, respectively. The project is not considered profitable if the net present worth is negative. In making the comparisons of the investments, the larger the NPV, the more favorable the investment.

2.3.3. Discounted Cash Flow Rate of Return

The discounted cash flow rate of return (*DCFR*) also known as internal rate of return is the return on investment while considering the time value of money. It is obtained from an investment in which all the investment and cash flow are discounted [37]. The *DCFR* is estimated by setting the net present worth equal to zero and solving for the rate used in the present worth factors using Equation (16). If the *DCFR* exceeds the *WACC*, the project is considered profitable.

$$0 = \sum_{j=1}^{N} \left[(1 + DCFR)^{-j} \right] (A_j + rec_j) - \sum_{k=1}^{N_c} \left[(1 + DCFR)^{N_c - k} \right] ₮_k \tag{16}$$

2.3.4. Levelized Cost of Energy

The levelized cost of energy is the average cost of energy (USD/MW-h or USD cent/kW-h) produced over the lifetime of the plant and is calculated using Equation (17) where E_j is the energy produced each year. For this study, the *LCOE* is the combined cost of total electricity and thermal energy produced. It is also defined as "the discounted lifetime cost of ownership and usage of a generation asset, transformed into a USD/MWh equivalent unit of cost of generation". The energy produced is discounted in *LCOE* calculations [39]. When comparing different investments or technologies, *LCOE* is the best tool to employ as it measures the competitiveness of the technology [39]. Less competitive technology is characterized by a higher value of *LCOE*.

$$LCOE = \frac{\sum_{j=1}^{N} PWF_{cf,j}(c_{o,j}) + \sum_{k=1}^{Nc} PWF_{v,k} ₮_k}{\sum_{j=1}^{N} PWF_{cf,j} E_j} \tag{17}$$

2.4. Study Approach and Assessment Scenarios

To study the techno-economic analysis of the advanced SMR and SMR-ChHP systems, the utility data from U.S. Energy Information Administration (EIA) [40] for six different regions (California, Northwest, Midwest, Southwest, New England, and PJM) of United States were used as shown in Table 2. The values were averaged for industrial gas prices and electricity data for the year 2021.

Table 2. Utility Data for Different Regions.

Region	2021 Industrial Natural Gas Price (USD/MMBtu)	2021 Electricity Data (USD/MWh)
California	9.06	66.5
Midwest	6.07	57.7
Northwest	8.15	59.78
New England	9.68	47.75
Southwest	5.62	64.78
PJM	6.67	42.55

For this study, advanced SMR with thermal output 100 MW_{th} is assumed. For the techno-economic analysis, different scenarios are considered based on the different thermal output of ChHP as shown in Figure 6 for an ideal case (*CF* = 100%). The first scenario is when the 100 MW_{th} advanced SMR sells electricity with a power conversion efficiency of 34% is represented as SMR. The second scenario is an NHES where a 100 MW_{th} advanced SMR coupled with a 50 MW_{th} output ChHP with coefficient of performance (COP) of 0.58, which sells heat, and rest of the energy from SMR sells electricity, which is represented as NHES-1. In the third scenario, NHES-2, an advanced SMR is coupled with a 10 MW_{th} output ChHP, which offers heat and rest of the energy from SMR produces electricity. The fourth and fifth scenarios where NHES-3 and NHES-4, which include an advanced SMR coupled with a 5 and 1 MW_{th} output ChHP, respectively.

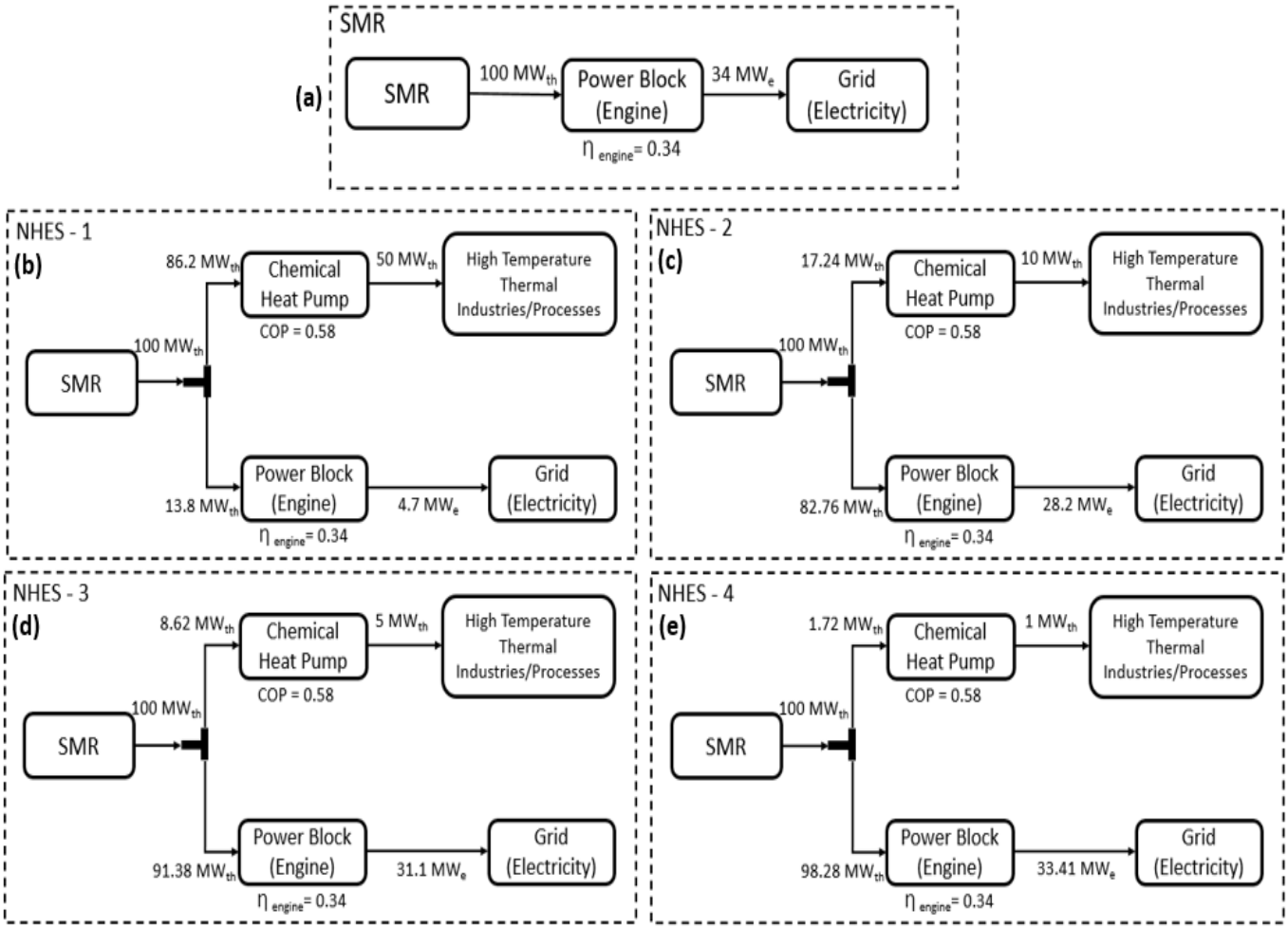

Figure 6. Advanced SMR and SMR-ChHP combined scenarios (**a**) base case SMR generating electricity; (**b**–**e**) SMR-ChHP coupled system generating heat and electricity in different proportions.

For conducting the economic analysis, the economic parameters assumed from the literature are listed in Table 3. A parametric study based on different overnight capital cost of advanced SMR, and carbon taxes is also conducted.

Table 3. Parameters Assumed for this Study.

Parameters	Assumed Values	References
Overnight Cap Cost	USD4637/kW_e	Sabharwall et al. [29]
Capacity Factor	90%	Sabharwall et al. [29]
Lifetime	60 years	Sabharwall et al. [29], Alonso et al. [30]
Variable O&M Cost	USD0.486/MWh_e	Sabharwall et al. [29]
Fixed O&M Cost	USD19,500,000/year	Sabharwall et al. [29]
Fuel Cost	USD0 (included in O&M)	Sabharwall et al. [29]
Construction Period	3 (60%, 20%, 20%)	Alonso et al. [30]
CO_2 Tax	USD150/ton	Locatelli et al. [41]
Depreciation	Variable	MACRS Method [37]
Corporate Tax Rate	21%	Nuclear Energy Institute [42]
Inflation Rate	1.1%	MIT report [3]
Cost of Debt	4%	Sabharwall et al. [29]
Debt Portion	30%	Sabharwall et al. [29]

3. Results and Discussion

In this study, based on the economic input assumptions the calculated discount rate (*i*) is 3.552%, the cost of equity is 4.84% and the *WACC* is estimated to be 4.588%. The ChHP specific capital cost was estimated as USD4500/kW based on thermal model for baseline system and CG Thermal [35] specific chemical bed cost assumption. These calculated values were used to determine the economic parameters and profitability of the different scenarios between advanced SMR and SMR-ChHP systems.

3.1. Economic Indicators Analysis

Based on the utility prices assumed for six different U.S. regions, economic indicators for SMR, NHES-1, NHES-2, NHES-3, and NHES-4 were evaluated as described in Section 2.4. Figure 7 shows the NPV values of advanced SMR and SMR-ChHP output scenarios. All the nuclear hybrid energy systems have higher NPV values then SMR for every region because of higher sales revenue. As per NPV estimates, it is observed that selling heat from NHES-1 with a 50 MW_{th} output is most profitable compared to lower thermal output ChHP or selling electricity from a 100 MW_{th} advanced SMR. New England and PJM regions NPV values of USD162 and USD251.8 million shows the best case for selling heat for high temperature industrial processes because of their high natural gas and low electricity prices as per the percentage increase in NPV values compared to an SMR in their region.

Figure 8 shows the payback period (PBP) of advanced SMR and SMR-ChHP output scenarios and Figure 9 shows the percentage deviation of PBP for different NHES systems from advanced SMR values. The New England and PJM regions showed shorter payback periods of 16.4 and 19.12 years, respectively, NHES-1 makes the most profitable scenario for selling heat at higher scale whereas for other regions PBP for NHES-1 system were higher. NHES-2, 3, and 4 showed slightly lower PBP from advanced SMR values in California, Midwest, Northwest, and Southwest regions. NHES-4 is the most profitable case in California, Midwest, Northwest, and Southwest regions as the PBP period is the lowest among NHES-2, 3 and advanced SMR asserting that SMR-coupled with 1 MW_{th} ChHP system providing heat and electricity is always more profitable than an advanced SMR selling electricity only in terms of PBP. The negative percentage deviation in Figure 10 shows the PBP of NHES system is lower than advanced SMR values making system profitable. Except NHES-1 in California, Midwest, Northwest, and Southwest regions and NHES-2 in Southwest has positive percentage deviation from SMR values favoring SMR despite the fact that the ChHP has higher sales income and NPV values, the NPV is

computed by making an assumption of 60-year plant life, which means after the capital cost is recovered there are many years to earn a profit.

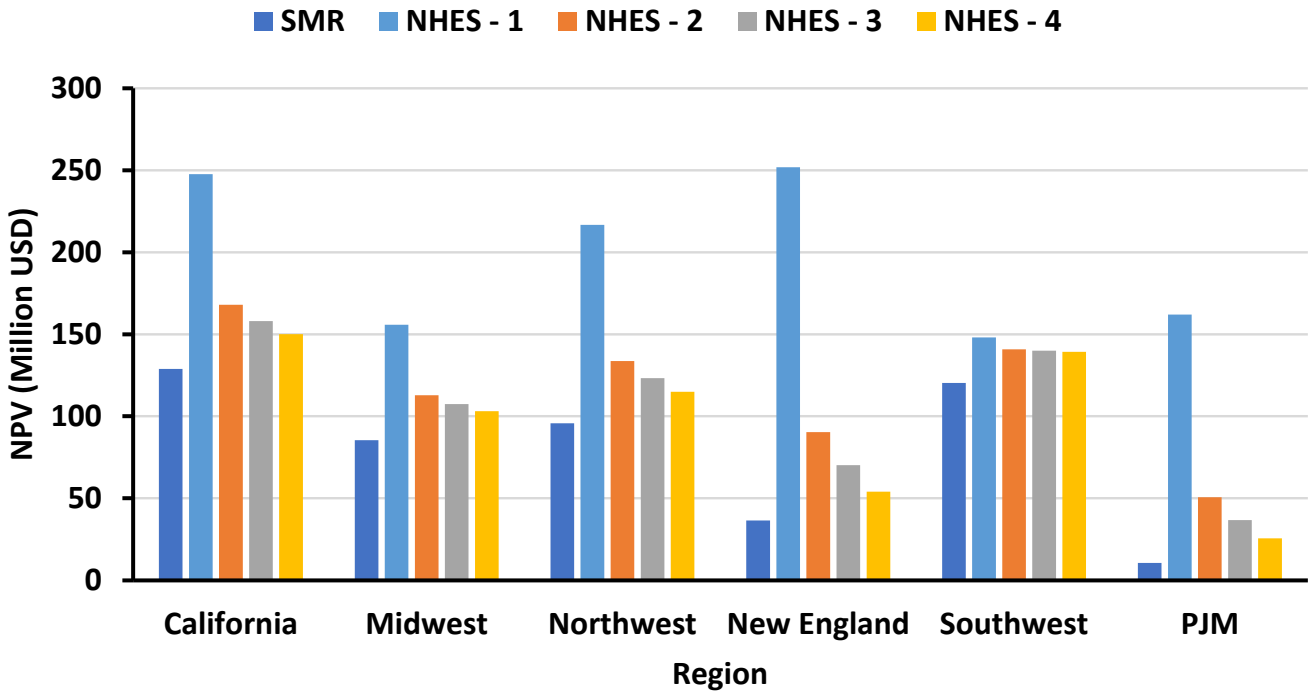

Figure 7. NPV values at different regions for SMR and different SMR-ChHP output scenarios.

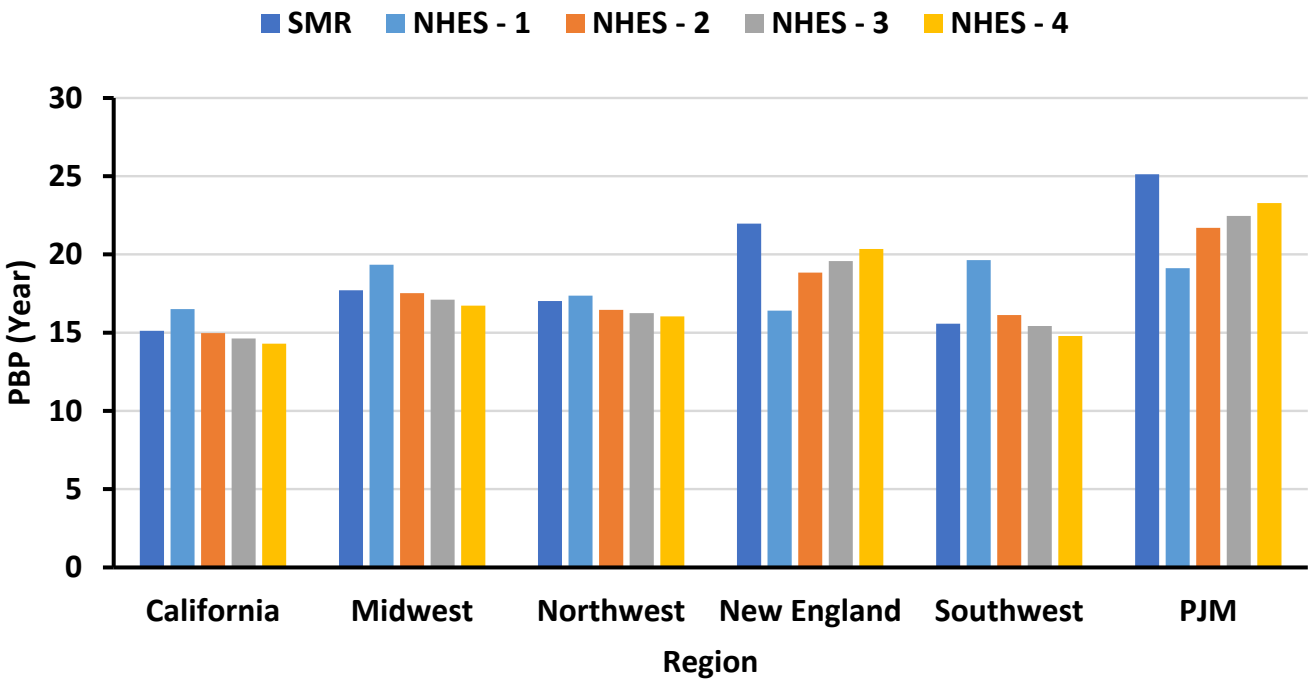

Figure 8. PBP at different regions for SMR and different SMR-ChHP output scenarios.

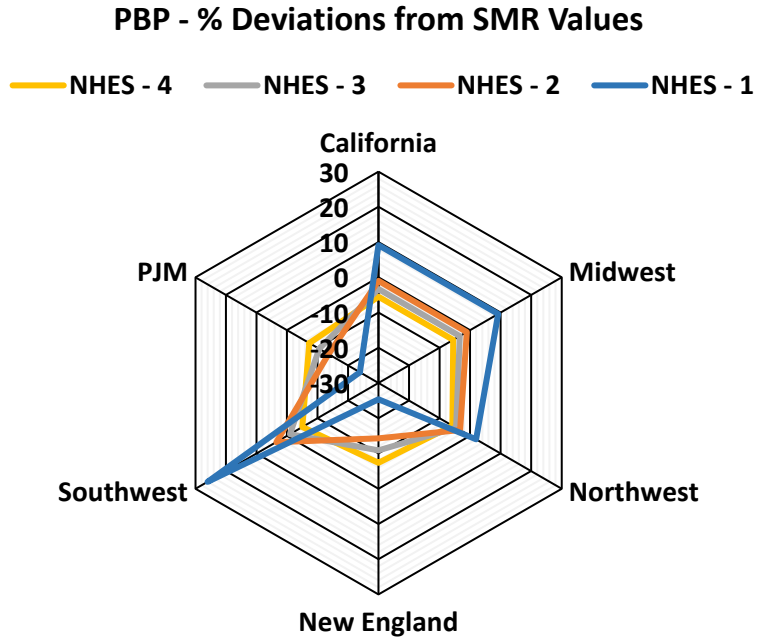

Figure 9. Percentage deviation of PBP for different NHES scenarios from SMR values.

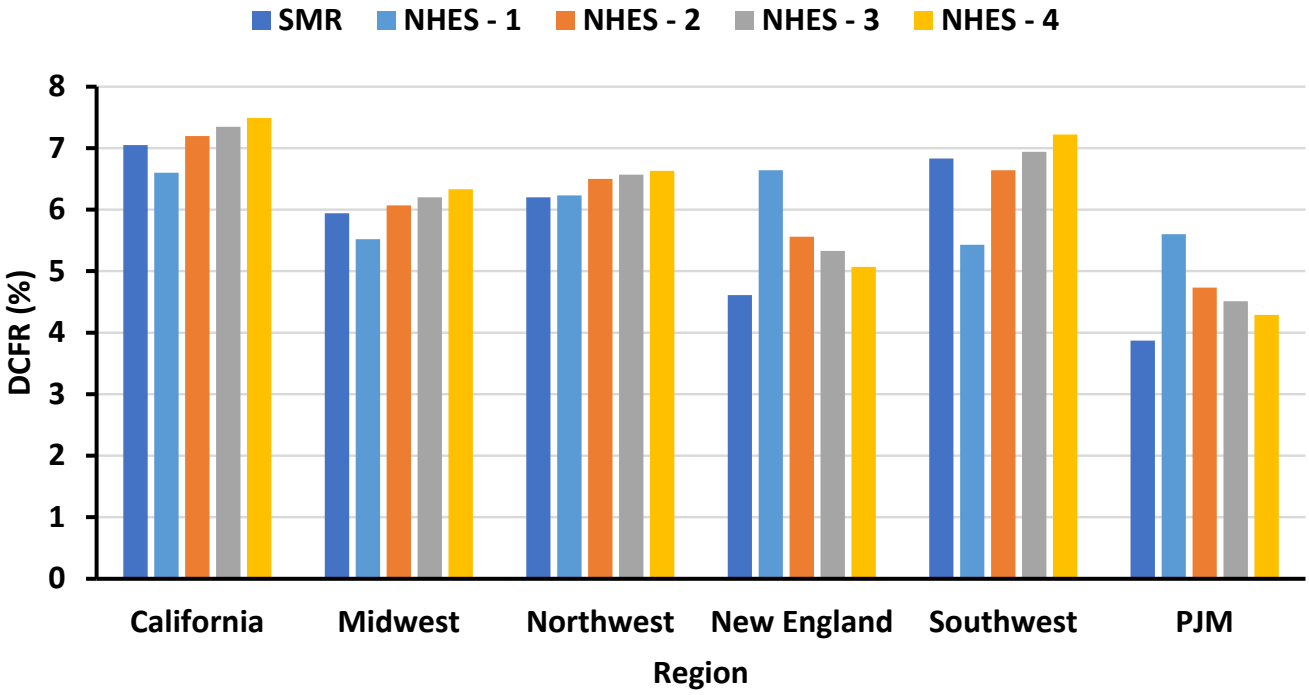

Figure 10. DCFR at different regions for SMR and different SMR-ChHP output scenarios.

The DCFR calculations are shown in Figure 10, and all the NHES systems have DCFR values greater than WACC asserting the project is acceptable, and then it should be compared with other accepted scenarios or projects as per Bolden 2015. The DCFR values for New England and PJM are significant higher for NHES-1 system compared to advanced SMR making it the most profitable case for selling heat. Figure 11 shows the percentage deviation of DCFR for different NHES systems from advanced SMR values. The four cases where DCFR values of NHES systems are less than advanced SMR values are California, Midwest and Southwest for NHES-1 system and NHES-2 for southwest system. The DCFR

analysis also confirmed that SMR-ChHP system is always profitable at different regions based on different ChHP thermal output scenarios.

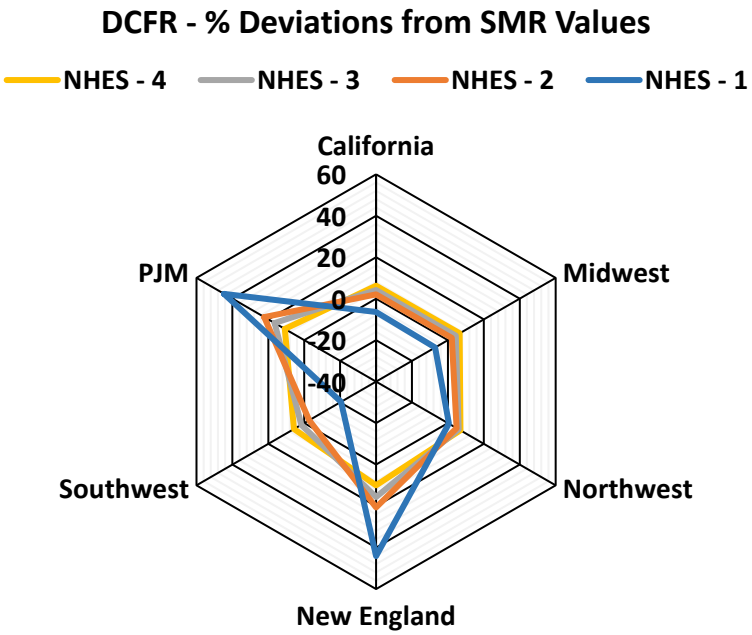

Figure 11. Percentage deviation of DCFR for different NHES scenarios from SMR values.

The Figure 12 shows the LCOE values for SMR and NHES systems for different scenarios. The LCOE for advanced SMR is 36.93 USD/MWh whereas the different coupled SMR-ChHP scenarios have LCOE values 23.85, 36.14, 38.62 and 40.88 USD/MWh for NHES-1, 2, 3, and 4, respectively. NHES-1 has lower LCOE when compared to advanced SMR making NHES-1 a better investment as SMR-ChHP system is producing more energy than advanced SMR and overcomes the cost of the coupled system well. NHES-2 has slightly higher LCOE value compared to advanced SMR signifying that selling heat and electricity via coupled system balances out the cost of SMR-ChHP. NHES-3 and 4 have higher LCOE as the cost of the system does not balances out the energy produced by the coupled system.

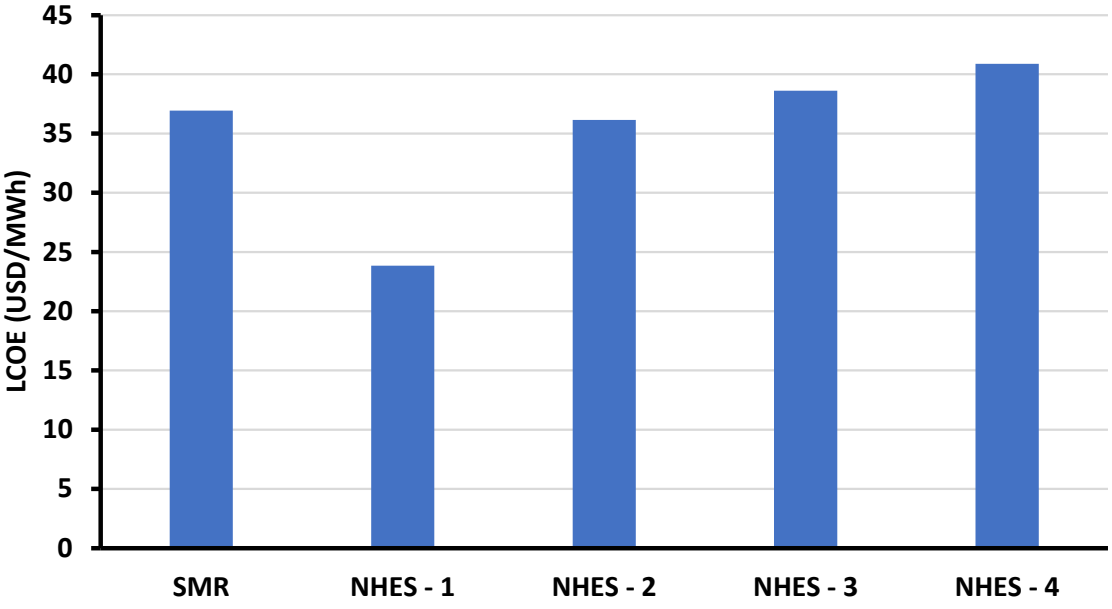

Figure 12. LCOE for SMR and different SMR-ChHP output scenarios.

Based on the above evaluated economic indicators for different U.S. region, NHES comparing of SMR coupled with ChHP showed that selling heat to high temperature industrial process and electricity to the grid makes advanced SMR more profitable and helps reduce the burning of fossil fuels to produce heat. In California, Midwest, Northwest, and Southwest it is more profitable to have NHES-3 or 4 compared to NHES-1 and 2 and advanced SMR based on PBP and DCFR values. Though based on high NPV values NHES-1 can also be considered. In PJM and New England, NHES-1 is more profitable based on their utility prices, asserting selling heat at higher scale is more cost-effective and favorable. Table 4 shows the profitable scenarios where the ChHP coupled system with advanced SMR would be profitable. As NPV of coupled system is always greater than advanced SMR, the PBP and DCFR is used to estimate the profitability. If DCFR of NHESs is greater than advanced SMR and PBP of NHESs is less than advanced SMR then NHESs system is considered profitable. In the Table below, 1 is most profitable and 5 is least profitable scenario. The four important factors the which affects the economics the most are: carbon taxes, overnight capital cost of SMR, ChHP capital cost and thermal conductivity based on previous work [31]. The sensitivity analysis based on carbon taxes and overnight capital cost of SMR is mentioned in section below.

Table 4. Table shows the profitable scenarios (1 being most profitable and 5 being least profitable) based on DCFR and PBP.

Regions	SMR	NHES-1	NHES-2	NHES-3	NHES-4
California	4	5	3	2	1
Midwest	4	5	3	2	1
Northwest	5	4	3	2	1
New England	5	1	2	3	4
Southwest	3	5	4	2	1
PJM	5	1	2	3	4

3.2. Parametric Study on Overnight Capital Cost of Advanced SMR

To access the economic competitiveness of advanced SMR and different SMR-ChHP systems, a parametric study on overnight capital cost of advanced SMR was conducted for the values ranging from USD4500/kW_e to USD6500/kW_e based on the diverse values reported in literature. The aim of this parametric study is to assess the effect on NPV and PBP of the proposed scenarios for different utility prices and U.S. regions. Advanced SMR, NHES-1 and NHES-2 will be the focus of this study based on results discussed in Section 3.1.

Figures 13–16 show the NPV and PBP values at different overnight capital cost of advanced SMR for California, Midwest, Northwest, and Southwest, respectively. As the overnight capital cost of advanced SMR is increased, the NPV of the SMR, NHES-1 and 2 decreased as expected. The PBP is increased for the SMR, NHES-1 and 2 as the overnight capital cost of advanced SMR is increased. For California, Midwest, Northwest, and Southwest regions, NPV of NHES-1 and 2 are still positive and higher than advanced SMR value when overnight capital cost of advanced SMR is increased from USD4500/kW_e to USD6500/kW_e.

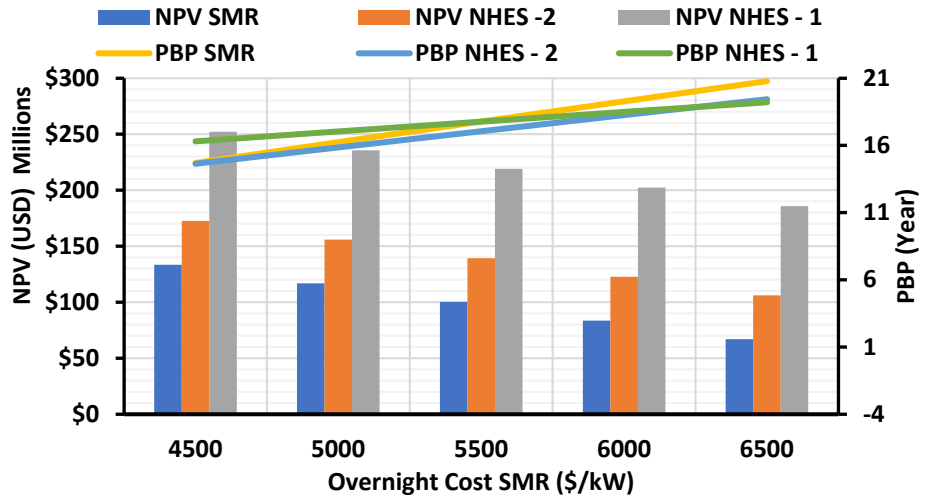

Figure 13. NPV and PBP vs. overnight cost of advanced SMR for California region.

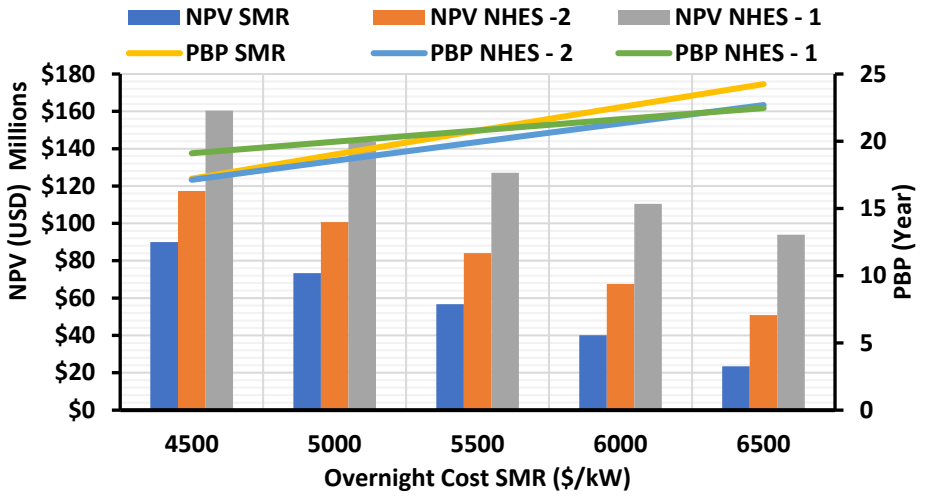

Figure 14. NPV and PBP vs. overnight cost of advanced SMR for Midwest region.

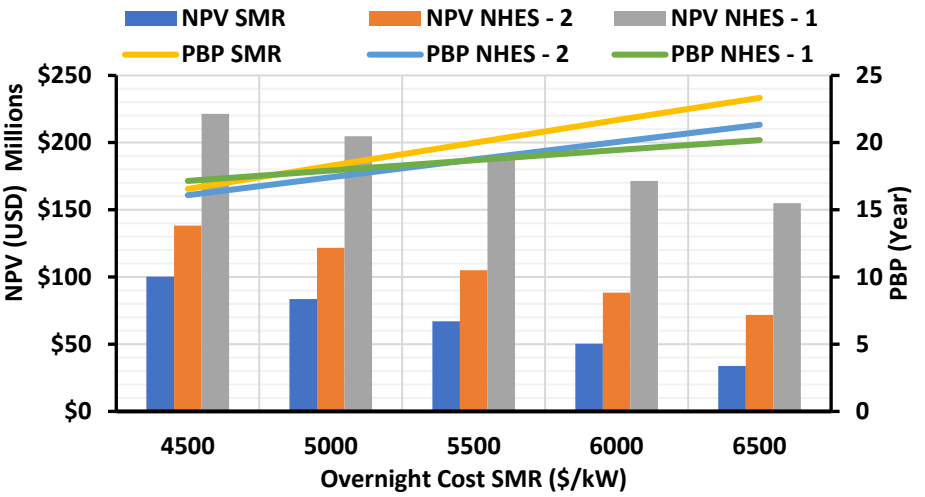

Figure 15. NPV and PBP vs. overnight cost of advanced SMR for Northwest region.

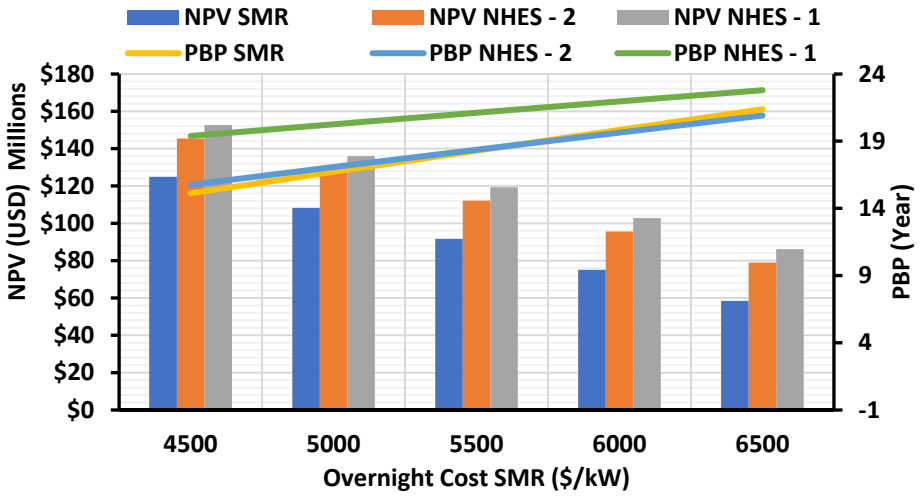

Figure 16. NPV and PBP vs. overnight cost of advanced SMR for Southwest region.

When the overnight capital cost of SMR exceeds USD5500/kW_e and USD6100/kW_e, respectively, the PBP for NHES-2 and NHES-1 starts to fall when compared to advanced SMR in California. Based on utility data from Midwest region, the PBP of NHES-2 and NHES-1 when compared with advanced SMR begins to reduce once the overnight capital cost of SMR is increased to USD4500/kW_e and USD5500/kW_e, respectively. The PBP for Northwest region was already less for NHES-1 when compared with SMR for USD4500/kW_e overnight capital cost. When the overnight capital cost is increased to USD4800/kW_e the NHES-1 system had less PBP then advanced SMR. The Southwest region, NHES-1 would not have lower PBP than advanced SMR based on assumed overnight capital cost. NHES-2 will have PBP lower than advanced SMR once the overnight capital cost is increased to USD5800/kW_e.

Figures 17 and 18 show the NPV and PBP values at different overnight capital cost of advanced SMR for New England and PJM, respectively. Based on New England and PJM utility prices, NHES-1 will always have lower PBP when compared with NHES-2 and advanced SMR with increased overnight capital cost though the individual system PBP value will increase. NPV of both the regions are significantly higher for NHES-1. If the overnight capital cost is increased above USD5500/kW_e and USD5000/kW_e for New England and PJM, respectively, then NPV of SMR will become negative making SMR not profitable. In this case, the system will be economically profitable if SMR is coupled with ChHP and sells heat and electricity.

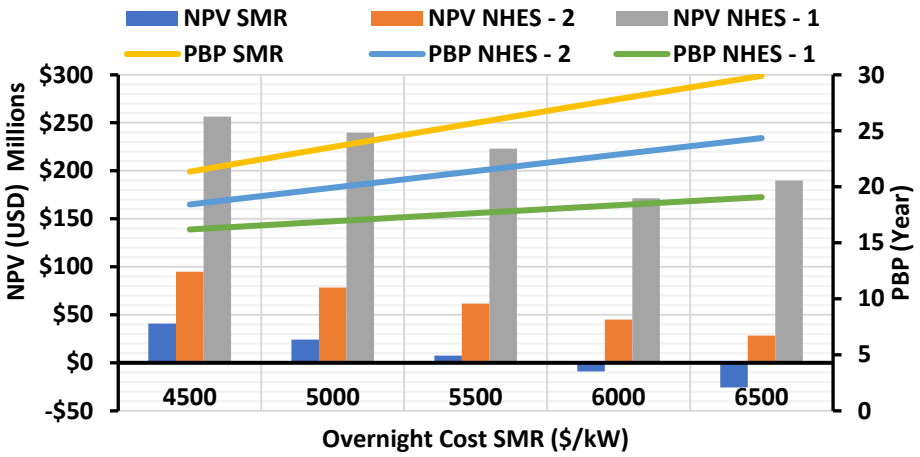

Figure 17. NPV and PBP vs. overnight cost of advanced SMR for New England region.

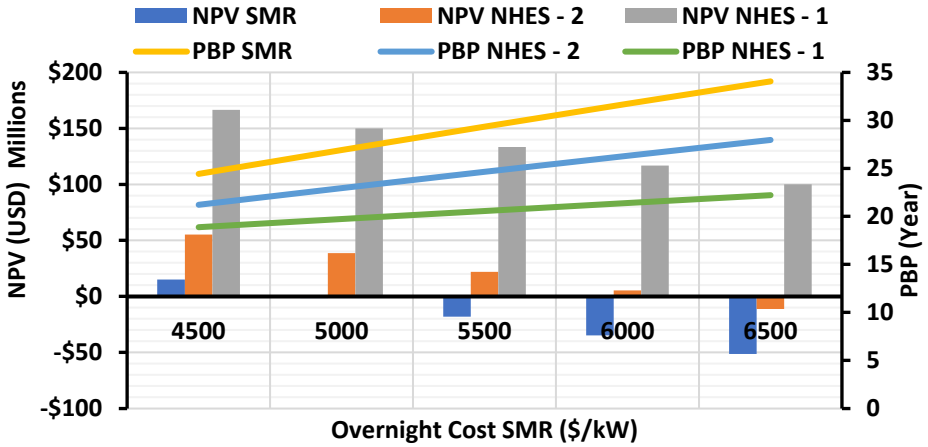

Figure 18. NPV and PBP vs. overnight cost of advanced SMR for PJM region.

3.3. Impact of Increased Carbon Taxes

In order to accomplish the goal of keeping global temperatures below 1.5 °C by 2030, which was discussed at COP26, the price of carbon tax should be higher. This tax reduces emissions by increasing the cost of carbon-based fuels to motivate the switch to clean energy technologies such as nuclear, solar, wind and hydro sources. Taxes will allow industries to find the most cost-effective way to reduce emissions. This study was conducted to analyze the impact of increased carbon taxes on PBP for NHES (SMR-ChHP) systems.

The two different carbon tax rates assumed in this study were USD150/ton (basis of analysis in Section 3.1) and USD200/ton. Different NHES scenarios are studied for different U.S. regions because the carbon tax rate impacts the value of heat. All other assumptions stated in Table 3 were unchanged except carbon tax. As NPVs of the NHES systems were significantly higher than advanced SMR for all the scenarios and cases, PBP was the focus of this study. For the California region, the difference in PBP with different carbon taxes are shown in Figure 19 for the different NHES configurations when compared with advanced SMR. When carbon tax of USD150/ton was assumed, PBP of NHES-1 increased by 1.4 years over that for the advanced SMR but as the carbon tax increased to USD200/ton the PBP decreased by 0.6 years for the same system from that of the advanced SMR. PBPs of NHES-2, 3, and 4 systems were further lowered than advanced SMR values when carbon tax was increased from USD150/ton to USD200/ton. Similar trend was followed by Midwest region as shown in Figure 20 where PBPs of NHES-2, 3 and 4 systems were further lowered than advanced SMR values when carbon tax was increased. NHES-1 had a 1.65 year longer payback period than SMR at USD150/ton carbon tax, but this value was decreased by 1 year when the carbon tax was raised to USD200/ton. If difference in PBP is negative, then the NHES system is more profitable when compared to advanced SMR.

For the Northwest region, the difference in PBP values for NHES-2, 3, and 4 were further lowered as excepted compared to SMR when carbon tax was increased as shown in Figure 21. However, the PBP for NHES-1 was 0.35 years higher than SMR for USD150/ton carbon tax but the PBP was decreased by 1.8 years from SMR when the carbon tax was increased to USD200/ton. In Southwest region as shown in Figure 22, even after increasing the carbon tax to USD200/ton, PBP of NHES-1 was still higher than advanced SMR value. However, PBP of NHES-2, 3, and 4 systems were lowered than SMR values with increased carbon tax.

The New England and PJM were the two most profitable cases for the NHES-1 system as per the study described in Section 3.1. Increasing the carbon tax rate has further lowered the difference in PBP from −5.6 years to −7.5 years and −6 years to −8.6 years from SMR values for New England and PJM regions, respectively, as shown in Figures 23 and 24.

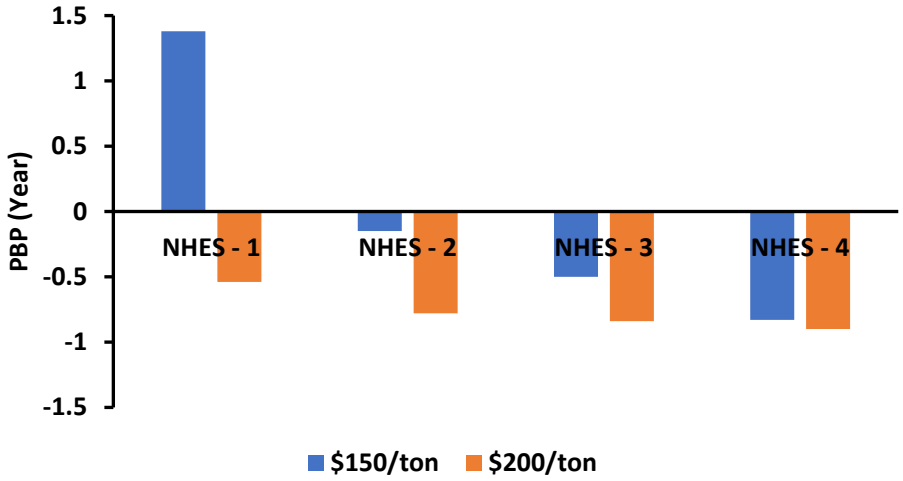

Figure 19. Difference in PBP based on increased carbon tax for California region.

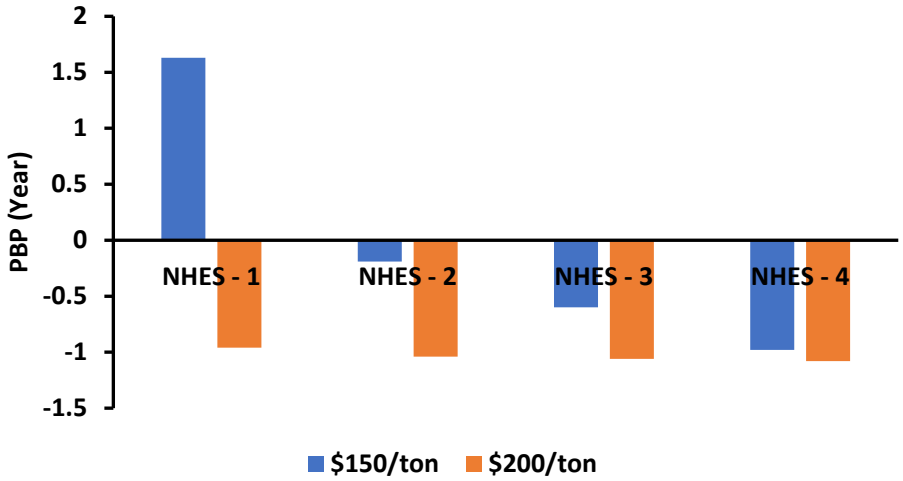

Figure 20. Difference in PBP based on increased carbon tax for Midwest region.

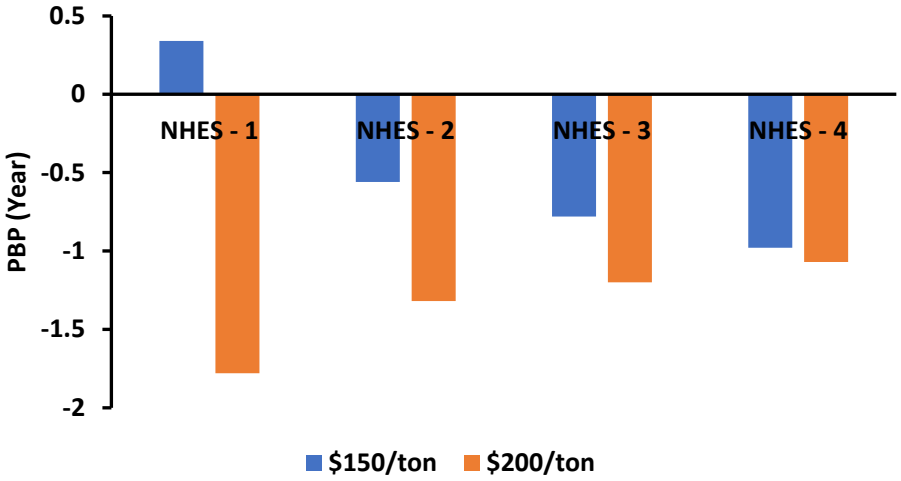

Figure 21. Difference in PBP based on increased carbon tax for Northwest region.

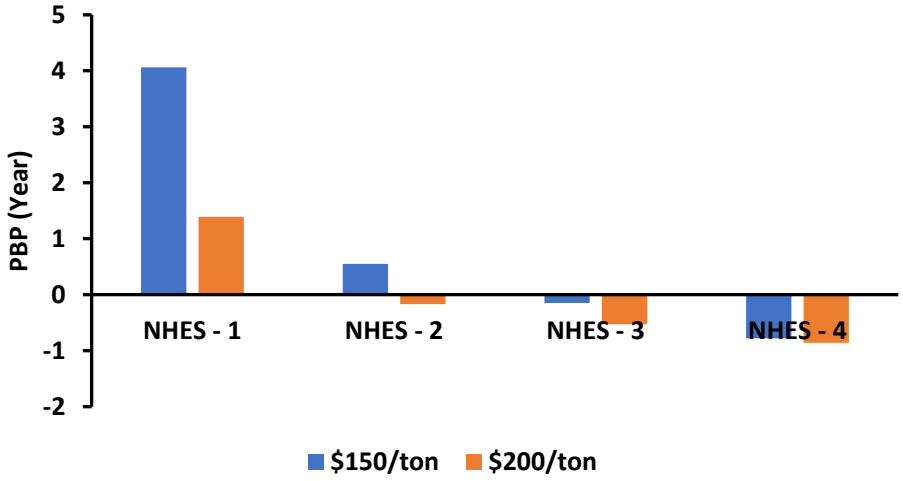

Figure 22. Difference in PBP based on increased carbon tax for Southwest region.

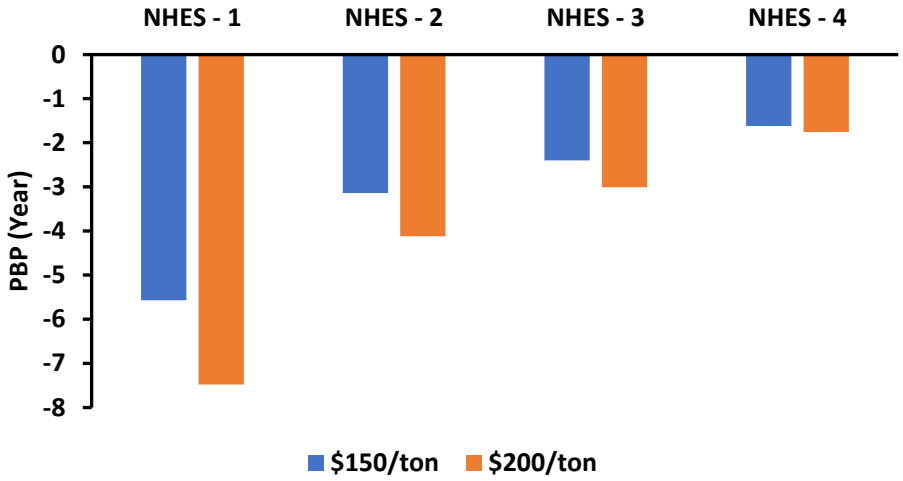

Figure 23. Difference in PBP based on increased carbon tax for New England region.

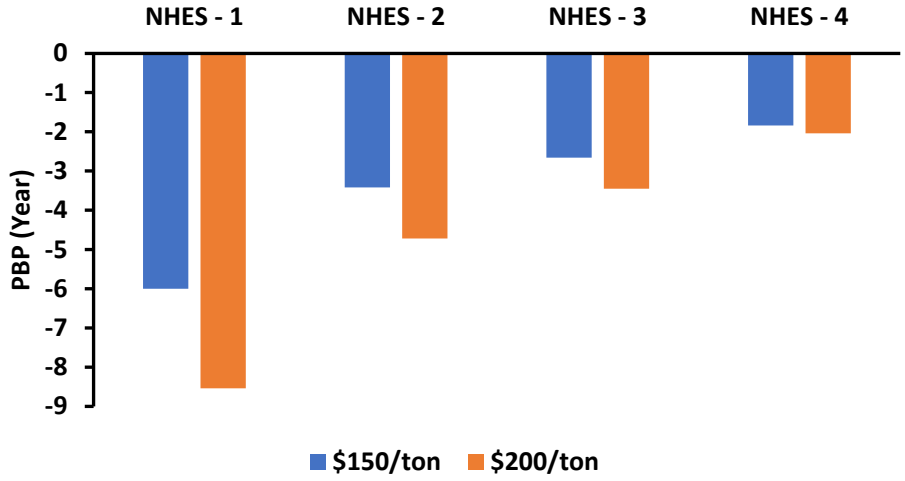

Figure 24. Difference in PBP based on increased carbon tax for PJM region.

The techno-economic analysis showed that the using ChHP for temperature amplification of nuclear heat increases the profit by selling heat. Higher overnight capital cost of advanced SMR favors the coupled SMR-ChHP system. A carbon tax would result in higher prices for carbon-intensive goods and services, potentially rewarding innovations,

and investment in clean energy technologies. Higher carbon tax on natural gas benefits the SMR-ChHP system by increasing NPV and reducing the DCFR and PBP values. A higher price of carbon emissions will encourage firms and consumers to develop more efficient clean energy technologies. Some of the countries in Europe started to implement carbon tax for more than USD100/ton. The US is unlikely to see such high carbon taxes in the near future, with most proposals seeking to impose carbon taxes around USD25–50/ton. For future consideration, a techno-economic analysis on hourly utility data for different U.S. regions will be valuable to understand the combination of electricity and high temperature heat produced. Further research and development on the ChHP and chemical bed design are essential to reduce down the specific capital cost of ChHP system. Market analysis on high temperature industrial power required is necessary to understand the possible scale of the system. Detailed analysis based on the variable peak demand is needed to divert the heat to the turbine and to study its effect on the economics of IES.

4. Conclusions

A techno-economic analysis was conducted for an advanced SMR and SMR coupled with different thermal output ChHP system to determine the profitability of selling heat in addition to electricity only. The analysis employed electricity and natural gas prices for six different U.S. regions (California, Northwest, Midwest, Southwest, New England, and PJM) based on EIA data. For this study, advanced SMR combined with ChHP was referred as NHES. Advanced SMR with 100 MW_{th} and four different scenarios of NHES were considered based on thermal output from ChHP i.e., 50-, 10-, 5-, and 1-MW_{th}, represented as NHES-1, 2, 3, and 4, respectively. The NPV, PBP, DCFR, and LCOE were evaluated for SMR and NHES systems. The economic analysis showed that selling heat and electricity from SMR-ChHP is most profitable in PJM and New England region based on utility prices of different regions. The parametric study on increasing overnight capital cost of advanced SMR indicated selling heat will be economically profitable than only selling electricity only. Increased carbon tax also resulted in significant improvements in economic indicators by selling heat. Providing heat to high temperature thermal industries could be a game changer for nuclear power and help achieve the climate change goal by reducing the burning of fossil fuel.

Author Contributions: Conceptualization, A.G., P.S., B.M.F. and V.U.; Data curation, A.G.; Formal analysis, A.G. and P.D.A.; Funding acquisition, B.M.F. and V.U.; Methodology, A.G. and P.D.A.; Project administration, V.U.; Supervision, P.S., B.M.F. and V.U.; Validation, P.S.; Writing—original draft, A.G. and P.D.A.; Writing—review and editing, P.S., B.M.F. and V.U. All authors have read and agreed to the published version of the manuscript.

Funding: U.S. Department of Energy Office of Nuclear Energy's Nuclear Energy University Program under Award Number DE-NE0008775.

Institutional Review Board Statement: Not applicable.

Informed Consent Statement: Not applicable.

Data Availability Statement: Not applicable.

Acknowledgments: This research is being performed using funding received from the DOE Office of Nuclear Energy's Nuclear Energy University Program under Award Number DE-NE0008775.

Conflicts of Interest: The authors declare no conflict of interest.

Nomenclature

$\overline{A}$	average annuity	USD
A	annuity	USD

A_{HT}	heat transfer area	m^2
C	rate	-
CC	contingency cost rate	-
CF	capacity factor	-
c_0	costs	USD
$DCFR$	discounted cash flow rate of return	-
$DD\&E$	detailed design and engineering rate	-
d	depreciation rate	-
E	energy	MWh
$Fuel_{spec}$	specific fuel cost	USD MW_e^{-1}
i	discount rate	-
k	thermal conductivity	W m^{-1} K^{-1}
$LCOE$	levelized cost of energy	USD MW^{-1} h^{-1}
L	length	m
NPV	net present worth	USD
N	time period	yr
n	number or magnitude	-
$O\&M_{fix}$	fixed operations and maintenance	USD $MW_e^{-1}yr^{-1}$
$O\&M_{spec}$	specific operation and maintenance	USD MW_e^{-1}
OCC	overnight capital cost	USD kW_e^{-1}
PBP	payback period	yr
PWF	present worth factor	-
p	portion	-
r	rate	-
rec	recovered cost from salvaged equipment	USD
SP	selling price of utility	USD MW^{-1} h^{-1}
SCC	specific capital cost	USD kW_e
₮	annual investment	USD
V	fixed capital investment	USD
$WACC$	weighted average capital cost	-
Greek Letters		
Δ	change or difference	-
η	first law thermodynamic efficiency	-
ϕ	tax rate	-
Subscript/Superscript		
bed	bed	
c	construction	
cf	annual cash flow	
d	debt	
eq	equity	
e	electricity	
inf	inflation	
j	plant operation year index	
k	plant construction year index	
th	thermal	
v	investment	
Abbreviations		
ChHP	Chemical Heat Pump	
EIA	Energy Information Administration	
FOAK	First-of-a-Kind	
GHG	Greenhouse gases	
IES	Integrated Energy System	
INRES	Integrated Nuclear-Renewable Energy Systems	
MACRS	Modified Accelerated Cost Recovery System	
NHES	Nuclear Hybrid Energy System	
NOAK	Nth-of-a-Kind	
SMR	Small Modular Reactor	

References

1. Bragg-Sitton, S.M.; Boardman, R.; Rabiti, C.; O'Brien, J. Reimagining future energy systems: Overview of the US program to maximize energy utilization via integrated nuclear-renewable energy systems. *Int. J. Energy Res.* **2020**, *44*, 8156–8169. [CrossRef]
2. Bragg-Sitton, S.M.; Boardman, R.; Rabiti, C.; Kim, J.S.; McKellar, M.; Sabharwall, P.; Chen, J.; Cetiner, M.S.; Harrison, T.J.; Qualls, A.L. Nuclear-Renewable Hybrid Energy Systems: 2016 Technology Development Program Plan. 2016. Available online: https://doi.org/10.2172/1333006 (accessed on 21 November 2021).
3. MIT. The Future of Nuclear Energy in a Carbon-Constrained World. 2018. Available online: https://energy.mit.edu/research/future-nuclear-energy-carbon-constrained-world/ (accessed on 21 November 2021).
4. McMillan, C.A.; Boardman, R.; McKellar, M.; Sabharwall, P.; Ruth, M.; Bragg-Sitton, S. Generation and Use of Thermal Energy in the U.S. Industrial Sector and Opportunities to Reduce its Carbon Emissions. 2016. Available online: https://doi.org/10.2172/1334495 (accessed on 21 November 2021).
5. Wongsuwan, W.; Kumar, S.; Neveu, P.; Meunier, F. A review of chemical heat pump technology and applications. *Appl. Therm. Eng.* **2001**, *21*, 1489–1519. [CrossRef]
6. Arjmand, M.; Liu, L.; Neretnieks, I. Exergetic efficiency of high-temperature-lift chemical heat pump (CHP) based on CaO/CO2and CaO/H2O working pairs. *Int. J. Energy Res.* **2013**, *37*, 1122–1131. [CrossRef]
7. Sabharwall, P.; Wendt, D.; Utgikar, V.P. Application of Chemical Heat Pumps for Temperature. 2013. Available online: https://doi.org/10.2172/1104502 (accessed on 21 November 2021).
8. Schaube, F.; Koch, L.; Wörner, A.; Müller-Steinhagen, H. A thermodynamic and kinetic study of the de- and rehydration of $Ca(OH)_2$ at high H_2O partial pressures for thermo-chemical heat storage. *Thermochim. Acta* **2012**, *538*, 9–20. [CrossRef]
9. Matsuda, H.; Ishizu, T.; Lee, S.K.; Hasatani, M. Kinetic Study of Ca (OH) _2/CaO Reversible Thermochemical Reaction for Thermal Energy Storage by Means of Chemical Reaction. *Kagaku Kogaku Ronbunshu* **1985**, *11*, 542. [CrossRef]
10. Dai, L.; Long, X.-F.; Lou, B.; Wu, J. Thermal cycling stability of thermochemical energy storage system $Ca(OH)_2$/CaO. *Appl. Therm. Eng.* **2018**, *133*, 261–268. [CrossRef]
11. Schmidt, M.; Gutierrez, A.; Linder, M. Thermochemical energy storage with $CaO/Ca(OH)_2$ – Experimental investigation of the thermal capability at low vapor pressures in a lab scale reactor. *Appl. Energy* **2017**, *188*, 672–681. [CrossRef]
12. Schmidt, M.; Szczukowski, C.; Roßkopf, C.; Linder, M.; Wörner, A. Experimental results of a 10 kW high temperature thermochemical storage reactor based on calcium hydroxide. *Appl. Therm. Eng.* **2014**, *62*, 553–559. [CrossRef]
13. Criado, Y.A.; Alonso, M.; Abanades, J.C.; Anxionnaz-Minvielle, Z. Conceptual process design of a $CaO/Ca(OH)_2$ thermochemical energy storage system using fluidized bed reactors. *Appl. Therm. Eng.* **2014**, *73*, 1087. [CrossRef]
14. Schaube, F.; Kohzer, A.; Schütz, J.; Wörner, A.; Müller-Steinhagen, H. De- and rehydration of $Ca(OH)_2$ in a reactor with direct heat transfer for thermo-chemical heat storage. Part A: Experimental results. *Chem. Eng. Res. Des.* **2013**, *91*, 856–864. [CrossRef]
15. Funayama, S.; Takasu, H.; Zamengo, M.; Kariya, J.; Kim, S.T.; Kato, Y. Composite material for high-temperature thermochemical energy storage using calcium hydroxide and ceramic foam. *Energy Storage* **2019**, *1*, e53. [CrossRef]
16. Gupta, A.; Armatis, P.D.; Sabharwall, P.; Fronk, B.M.; Utgikar, V. Thermodynamics of $Ca(OH)_2$/CaO reversible reaction: Refinement of reaction equilibrium and implications for operation of chemical heat pump. *Chem. Eng. Sci.* **2021**, *230*, 116227. [CrossRef]
17. Gupta, A.; Armatis, P.D.; Sabharwall, P.; Fronk, B.M.; Utgikar, V. Energy and exergy analysis of $Ca(OH)_2$/CaO dehydration-hydration chemical heat pump system: Effect of reaction temperature. *J. Energy Storage* **2021**, *39*, 102633. [CrossRef]
18. Criado, Y.A.; Alonso, M.; Abanades, J.C. Enhancement of a $CaO/Ca(OH)_2$ based material for thermochemical energy storage. *Sol. Energy* **2016**, *135*, 800–809. [CrossRef]
19. Yan, J.; Zhao, C. First-principle study of $CaO/Ca(OH)_2$ thermochemical energy storage system by Li or Mg cation doping. *Chem. Eng. Sci.* **2014**, *117*, 293–300. [CrossRef]
20. Sakellariou, K.G.; Karagiannakis, G.; Criado, Y.A.; Konstandopoulos, A.G. Calcium oxide based materials for thermochemical heat storage in concentrated solar power plants. *Sol. Energy* **2014**, *122*, 215–230. [CrossRef]
21. Roßkopf, C.; Haas, M.; Faik, A.; Linder, M.; Wörner, A. Improving powder bed properties for thermochemical storage by adding nanoparticles. *Energy Convers. Manag.* **2014**, *86*, 93–98. [CrossRef]
22. Roßkopf, C.; Afflerbach, S.; Schmidt, M.; Görtz, B.; Kowald, T.; Linder, M.; Trettin, R. Investigations of nano coated calcium hydroxide cycled in a thermochemical heat storage. *Energy Convers. Manag.* **2015**, *97*, 94–102. [CrossRef]
23. Gupta, A.; Armatis, P.D.; Sabharwall, P.; Fronk, B.M.; Utgikar, V. Kinetics of $Ca(OH)_2$ decomposition in pure $Ca(OH)_2$ and $Ca(OH)_2$-$CaTiO_3$ composite pellets for application in thermochemical energy storage system. *Chem. Eng. Sci.* **2021**, *246*, 116986. [CrossRef]
24. Spoelstra, S.; Haije, W.; Dijkstra, J. Techno-economic feasibility of high-temperature high-lift chemical heat pumps for upgrading industrial waste heat. *Appl. Therm. Eng.* **2002**, *22*, 1619–1630. [CrossRef]
25. Karaca, F.; Kıncay, O.; Bolat, E. Economic analysis and comparison of chemical heat pump systems. *Appl. Therm. Eng.* **2002**, *22*, 1789–1799. [CrossRef]
26. Bayon, A.; Bader, R.; Jafarian, M.; Fedunik-Hofman, L.; Sun, Y.; Hinkley, J.; Miller, S.; Lipiński, W. Techno-economic assessment of solid–gas thermochemical energy storage systems for solar thermal power applications. *Energy* **2018**, *149*, 473–484. [CrossRef]
27. Boldon, L. PhD Thesis, Rensselaer Polytechnic Institute. 2015. Available online: https://ui.adsabs.harvard.edu/abs/2015PhDT.....258B (accessed on 1 March 2022).

28. Boldon, L.M.; Sabharwall, P. Small modular reactor: First-of-a-Kind (FOAK) and Nth-of-a-Kind (NOAK) Economic Analysis. 2014. Available online: https://www.osti.gov/biblio/1167545/ (accessed on 1 March 2022).
29. Sabharwall, P.; Bragg-Sitton, S.; Boldon, L.; Blumsack, S. Nuclear Renewable Energy Integration: An Economic Case Study. *Electr. J.* **2015**, *28*, 85–95. [CrossRef]
30. Alonso, G.; Bilbao, S.; del Valle, E. Economic competitiveness of small modular reactors versus coal and combined cycle plants. *Energy* **2016**, *116*, 867–879. [CrossRef]
31. Armatis, P.D.; Sabharwall, P.; Gupta, A.; Utgikar, V.; Fronk, B.M. Transient Effects and Material Challenges in Developing Chemical/Absorption Heat Pumps for Nuclear Energy Thermal Storage and Upgrade. *Energy Resour. Technol.* **2022**. *Submitted*.
32. Richards, J.; Sabharwall, P.; Memmott, M. Economic comparison of current electricity generating technologies and advanced nuclear options. *Electr. J.* **2017**, *30*, 73–79. [CrossRef]
33. Stewart, W.; Shirvan, K. Capital cost estimation for advanced nuclear power plants. *Renew. Sustain. Energy Rev.* **2022**, *155*, 111880. [CrossRef]
34. Armatis, P.D.; Gupta, A.; Sabharwall, P.; Utgikar, V.; Fronk, B.M. A chemical-absorption heat pump for utilization of nuclear power in high temperature industrial processes. *Int. J. Energy Res.* **2021**, *45*, 14612–14629. [CrossRef]
35. CG Thermal, Graphite & SIC Heat Exchangers | Fluoropolymers. Available online: https://cgthermal.com/ (accessed on 1 March 2022).
36. Linder, M.; Roßkopf, C.; Schmidt, M.; Wörner, A. Thermochemical Energy Storage in kW-scale based on $CaO/Ca(OH)_2$. *Energy Procedia* **2014**, *49*, 888–897. [CrossRef]
37. Peters, M.S.; Timmerhaus, K.; West, R.E. *Plant Design and Economics for Chemical Engineers*, 5th ed.; McGraw-Hill: New York, NY, USA, 2003.
38. IRS. How to Depreciate Property. Available online: https://www.irs.gov/publications/p946 (accessed on 1 March 2022).
39. Aldersey-Williams, J.; Rubert, T. Levelised cost of energy—A theoretical justification and critical assessment. *Energy Policy* **2018**, *124*, 169–179. [CrossRef]
40. EIA, U.S. EIA, U.S. Energy Information Administration. Available online: https://www.eia.gov/index.php (accessed on 1 March 2022).
41. Locatelli, G.; Bingham, C.; Mancini, M. Small modular reactors: A comprehensive overview of their economics and strategic aspects. *Prog. Nucl. Energy* **2014**, *73*, 75–85. [CrossRef]
42. Nuclear Energy Institute. Cost Competitiveness of Micro-Reactors for Remote Markets. Available online: https://www.nei.org/resources/reports-briefs/cost-competitiveness-micro-reactors-remote-markets (accessed on 1 March 2022).